Available online at BCREC website: https://bcrec.id

Bulletin of Chemical Reaction Engineering & Catalysis, 18 (2) 2023, 303-314

Research Article

Optimization of Discharge Plasma Reactor for Dry Reforming of Methane using Response Surface Methodology

Nabil Majd Alawi[1,*], Hassan H. Al-Mohammedawi[2], Firas Khaleel AL-Zuhairi[1], Hoang M. Nguyen[3], Jamal M. Ali[1]

[1]*Chemical Engineering Department, Chemical Engineering Department, University of Technology-Iraq, Baghdad, Iraq.*
[2]*Biochemical Engineering Department, Al-Khwarizmi College of Engineering, University of Baghdad, Baghdad, Iraq.*
[3]*Department of Chemical Engineering, University of Science and Technology, the University of Danang, 54 Nguyen Luong Bang st, Danang, 550000, Vietnam.*

Received: 25th May 2023; Revised: 18th July 2023; Accepted: 19th July 2023
Available online: 27th July 2023; Published regularly: August 2023

Abstract

This research provides a study of the dry reforming of methane (DRM), which converts two main greenhouses gases (CO_2 and CH_4) to synthesis gas (H_2 and CO) by a Dielectric Barrier Discharge (DBD) plasma reactor at atmospheric pressure. The Box-Behnken Design (BBD) method based on the Response Surface Methodology (RSM) was applied to determine the optimum experimental conditions on the plasma stability and the synthesis gas production. The synergistic effects of input power (P), CO_2/CH_4 ratio (R), and flow rate (FR) on the CO_2, CH_4 conversions, H_2, CO yields, and the syngas ratio of H_2 to CO were studied. With the desirability value of 0.97, the optimum values of 10.05 W (P), 1.03 (R), and 1.58 $L.min^{-1}$ FR were identified with CO_2 conversion of 48.56% and CH_4 conversion of 86.67%; H_2 and CO yields of 45.87% and 39.43% respectively; and syngas ratio of H_2 to CO of 0.88. The study shows that both P and FR have a major significant effect on the reactant conversions and syngas ratio, followed by R. Meanwhile, the value of R has a significant impact on the H_2, CO yields followed P and FR. In contrast, the synergistic effects between P-R, P-FR, and R-FR had a weak significant on the CO_2 and CH_4 conversions, H_2 and CO yields, and H_2 to CO ratio respectively. The quadratic term coefficients of P, R, and FR had a remarkable effect on all responses. Thus, the synergistic effect of the most important parameters improves the process efficiency.

Keywords: Design of Experiments; Response Surface Methodology; CO_2 reforming of methane optimization; Dielectric Barrier Discharge Plasma; Syngas production

How to Cite: N.M. Alawi, H.H. Al-Mohammedawi, F.K. AL-Zuhairi, H.M. Nguyen, J.M. Ali (2023). Optimization of Discharge Plasma Reactor for Dry Reforming of Methane using Response Surface Methodology. *Bulletin of Chemical Reaction Engineering & Catalysis*, 18(2), 303-314 (doi: 10.9767/bcrec.18320)

Permalink/DOI: https://doi.org/10.9767/bcrec.18320

1. Introduction

Due to the high energy consumption and rapid population growth, there are now environmental problems due to Green House Gases (GHG) release Methane and carbon dioxide are major contributors to global warming and climate change, making up a sizeable portion of GHG [1,2]. Many technologies and methods are used to create synthesis gas from CH_4 and CO_2 [3]. Chemical engineers use synthesis gas (H_2 + CO) as a starting point for the Fischer-Tropsch Synthesis (FTS) of a variety of fuels and chemicals, including dimethyl, methanol, and diesel

* Corresponding Author.
Email: nabil.m.alawi@uotechnology.edu.iq (N.M. Alawi)

fuel, as well as other value-added chemicals [4–6].

Gas phase reactions can be induced in an unusual way thanks to plasma technology. Methane and carbon dioxide have been transformed into synthesis gas using a variety of plasma dry reforming techniques, such as thermal plasma and non-thermal plasma discharge [7,8]. Synthesis gas produced by the steam reformation of methane gas ($CH_4 + H_2O \rightarrow CO + 3H_2$) [9], dry reformation of methane gas ($CH_4 + CO_2 \rightarrow 2CO + 2H_2$) [10],partial oxidation of methane ($2CH_4 + O_2 \rightarrow 2CO + 4H_2$) [11]. POM produces synthesis gas with a ratio of H_2 to CO) equals 2.0 that is a sensible ratio for (F-T) synthesis [12]. SRM generates synthesis gas with a ratio of H_2 to CO equals 3.0, but SRM creates synthesis gas with a ratio of H_2 to CO equals 3.0. But DRM delivers syngas with a ratio close to 1 that is preferable for use as an intermediate in oxygenated chemical synthesis and hydrocarbon synthesis. Despite this, DRM is more optimistic than other reforming methods due to its use of CO_2, one of the primary factors contributing to global warming [13].

DRM demonstrated its superiority over other methane reforming processes by producing synthesis gas using greenhouse gases rather than releasing them into the atmosphere [14]. The use of plasma DRM is thought to be the most efficient method of obtaining a high conversion for CO_2, CH_4, and synthesis gas selectivity [6]. There are two primary processes used in dry reforming, namely thermal plasma and cold plasma discharge. Cold plasma can reform CH_4-CO_2 through a variety of methods including DBDs, Corona Discharges (CDs), Atmospheric pressure glow discharges (APGDs), Gliding Arc Discharges (GADs), MW Discharges (MWDs), and Spark Discharges [15]. The thermal method includes Alternating Current (AC), arc torch Direct Current (DC), and radio frequency (RF) [16].

The Design of Experiments (DoE) is an important tool for optimizing processes since multi-input factors can be processed to determine how each factor influences process performance individually and together in the form of a single or multiple output response, thereby reducing the experiments number compared to traditional experiments with just single factor at a time [17,18]. Response Surface Methodology (RSM) is a very useful experimental design methodology for establishing the relationship between output responses and multiple input parameters, allowing us to interpret the responses in three dimensions and using contours to better understand the impact of factors individually and their interactions on the responses. H_2 and CO yields, as well as the ratio of H_2/CO, are influenced by a number of factors in plasma DRM, including feed gas rate of flow, the ratio of CO_2/CH_4, discharge power, and residence time [19]. Since these parameters have no dependency on each another, it is necessary to take into account how they interact in order to optimize the plasma DRM procedure. The need for numerous experiments under various test conditions makes it time-consuming and expensive to determine the plasma process' optimal performance using standard experiments [20]. In our previous study, we developed an algorithm successfully [21,22]. The best value for output responses was found to be determined using the chemical model. Comparing this model to conventional methods, an importantly smaller number of experiments are needed [18]. To the best of the authors' knowledge, investigation of the synergistic impacts of main factors and finding of the optimum operating conditions for plasma stability and syngas production using DBD still requires more investigation and this has motivated the present work. Therefore, in the present study, a Box-Behnken design is employed to investigate the synergistic effects of the important factors including P, R, and FR using three levels and find their optimum values.

2. Materials and Methods

2.1 Procedure of Experiments

In this study, CH_4, CO_2 and N_2 gases with high purities of 99.99% were used. The schematic diagram of the experimental setup applied to produce syngas using plasma reactor was described previously [23]. The plasma reactor was injected with N_2 gas which was applied to generate the plasma flame. CH_4 and CO_2 were mixed with desired composition using

Table 1. Experimental range and levels of the independent factors in the Box-Behnken Design.

Factor	Lower level	Average	Higher level
Input Power [A] (W)	8	10	12
CO_2/CH_4 Ratio [B]	0.8	1	1.2
Flow Rate [C] ($L.min^{-1}$)	1.2	1.6	2

a gas mixer. Then, reactant gases were fed to plasma reactor. The product gases were analyzed by the GC/MSD. The values of measurements were represented with the average of three measurements to enhance the accuracy.

The function of independent variables expressed in Equation (1) is named as Response surface:

$$y = (x_1, x_2, x_3, \dots, x_n) \quad (1)$$

Where, the answer of the system is y, and x_i are the factors, which are the action variables. The objective is to maximize the variables of action known as factors and the response variable Y. The fact that the operating variables are continuous and subject to negligible error in experiments is a crucial presumption. Finding a good approximation of the real functional relationship between the response surface and the independent variables is necessary [24,25]. In this work, three variables were used in a 3-level Box-Behnken design (BBD) to examine how these variables interacted to affect the performance of H_2 and CO yields and the ratio of H_2 to CO. The conversions of CO_2, CH_4, the yields of H_2, CO, and the syngas ratio of H_2 to CO are influenced by three independent variables, which have been named as input power [A], the ratio of CO_2 to CH_4 [B], and feed flow rate [C]. As shown in Table 1, each independent process factor has 3 distinct levels that are lower level, average, and higher level.

A total of fifteen experiment runs worked randomly in BBD, including 3 repeated experiment runs, as see in Table 2. The Response surfaces were produced by Minitab-17 Statistical Software. The analysis of variance (ANOVA) is used to decide the models' capability and fitness. The F-test and adequate metrics like the coefficient of determination R^2 can be used to determine the models' statistical significance and each term within these models. By creating projected contour plots and 3-D surface plots, the impact of the process parameters was investigated.

3. Results and Discussion

3.1 DoE Analysis

The inputs and outputs values relationships are described based on DoE analysis in 5 equations see Table 2. The CH_4 and CO_2 Conversions (Y_1, Y_2); H_2 and CO Yields (Y_5, Y_6); and the ratio of H_2 to CO (Y_7) are presented below in Equations (2-6).

Table 2. Average test results of response variables with different combination of factors.

Run	Factors			Responses									
	A	B	C	1	2	3	4	9	10	11	12	13	14
	Input power (W)	CO_2/CH_4 Ratio	Flow Rate (L/ min)	Experimental of CH_4 conversion	Predicated of CH_4 conversion	Experimental of CO_2 conversion	Predicated of CO_2 conversion	Experimental of H_2 yield	Predicated of H_2 yield	Experimental of CO yield	Predicated of CO yield	Experimental of H_2/CO ratio	Predicated of H_2/CO ratio
1	8	0.8	1.6	44.55	40.58	25.65	23.92	22.51	19.90	23.51	22.54	0.36	0.36
2	8	1.2	1.6	75.45	70.57	40.65	38.28	37.52	34.36	33.85	32.40	0.68	0.59
3	12	0.8	1.6	62.34	67.21	34.14	36.51	29.74	32.89	29.5	30.94	0.51	0.58
4	12	1.2	1.6	43.54	47.50	25.76	27.48	22.50	25.10	23.41	24.37	0.42	0.42
5	10	0.8	1.2	39.66	38.87	24.67	23.63	23.71	21.69	21.74	20.70	0.35	0.28
6	10	1.2	1.2	53.23	53.35	29.52	29.13	27.89	26.42	27.21	26.65	0.42	0.43
7	10	0.8	2	65.51	65.38	34.25	34.63	31.80	33.27	31.57	32.12	0.55	0.53
8	10	1.2	2	60.41	61.19	33.43	34.46	33.20	35.21	28.43	29.46	0.39	0.45
9	8	1	1.2	18.97	23.72	13.56	16.31	3.51	8.13	15.32	17.32	0.12	0.18
10	12	1	1.2	53.32	49.22	29.94	28.60	26.54	25.40	25.8	25.38	0.49	0.46
11	8	1	2	60.52	64.61	34.55	35.88	32.58	33.71	31.89	32.30	0.54	0.56
12	12	1	2	47.43	42.67	28.14	25.38	24.82	20.19	26.62	24.62	0.41	0.34
13	10	1	1.6	79.55	80.36	46.71	47.55	42.47	43.35	34.49	35.31	0.81	0.82
14	10	1	1.6	81.24	80.36	48.67	47.55	44.12	43.35	36.15	35.31	0.83	0.82
15	10	1	1.6	80.29	80.36	47.28	47.55	43.46	43.35	35.31	35.31	0.82	0.82

$$Y_1 = -1506 + 139.1[A] + 773[B] + 598.7[C] - 4.192[A]^2 - 178.1[B]^2 - 115.8[C]^2 - 31.06[AB] - 14.83[AC] - 58.3[BC] \quad (2)$$

$$Y_2 = -842.9 + 76.04[A] + 483.2[B] + 320[C] - 2.490[A]^2 - 151[B]^2 - 69.03[C]^2 - 14.61[AB] - 7.12[AC] - 17.7[BC] \quad (3)$$

$$Y_3 = -842 + 86.2[A] + 361[B] + 321.7[C] - 2.821[A]^2 - 99.9[B]^2 - 63.8[C]^2 - 13.91[AB] - 9.62[AC] - 8.7[BC] \quad (4)$$

$$Y_4 = -487.6 + 43.39[A] + 285.3[B] + 192.4[C] - 1.26[A]^2 - 67.7[B]^2 - 33.56[C]^2 - 10.27[AB] - 4.92[AC] - 26.9[BC] \quad (5)$$

$$Y_5 = -17.96 + 1.427[A] + 11.05[B] + 7.39[C] - 0.0456[A]^2 - 3.62[B]^2 - 1.547[C]^2 - 0.2562[AB] - 0.1563[AC] - 0.719[BC] \quad (6)$$

As shown in Table 3, the values of adjusted R^2 and predicted R^2 for CH_4 conversion are 0.9455 and 0.9275, respectively, for CO_2 conversion are 0.9129 and 0.9039, respectively, for H_2 yield are 0.9278 and 0.9088, respectively, for CO yield are 0.9004 and 0.8940, respectively, and for H_2/CO ratio are 0.9206 and 0.9132 respectively. The difference between the adjusted R^2 and predicted R^2 is less than 0.2. This indicates a high degree of correlation between the actual and predicted values.

To assess the significancy and suitability of the quadratic models, ANOVAs were used (Tables from 4 to 8). The CH_4 conversion equals 0.96, CO_2 conversion equals 0.97, H_2 yield equals 0.95, CO yield equals 0.96 and the ratio of H_2 to CO equals 0.94 were the coefficients of determination (R^2), as shown in Table 3. Because R^2 is close to 1, as shown in Figure 1(a-e), the relation between the responses and the variables that represented by the 2nd order equation, and there is an acceptable matching between the experimental and the predicted values.

3.2 Analysis of Variance (ANOVA)

The ANOVA for the 2nd order polynomial equations and significance, interactive, quadratic, and adequacy terms of the progression equations are presented in Tables 4 to 8. The level of importance of each term of fitting models was indicated by p-value. The impact is considered remarkable if p-value less than 0.05, the factor has a significant impact on the response, while if p-value is higher than 0.05 the factor has no significant effect on the response.

Tables 4 to 8 show that the linear term coefficients (A and C) significantly influenced the CO_2 and CH_4 conversions and H_2/CO ratio; while the linear term coefficient (B) was identified as significant parameters in the H_2, CO yields. In contrast, the quadratic term coeffi-

Table 3. Fit statistics for CH_4, CO_2 conversions; H_2, CO yields and H_2/CO ratio.

Parameter	R^2	Adjusted R^2	Predicted R^2
CH_4 Conversion	0.9627	0.9455	0.9275
CO_2 Conversion	0.9689	0.9129	0.9039
H_2 Yield	0.9485	0.9278	0.9088
CO Yield	0.9609	0.9004	0.8940
H_2/CO Ratio	0.9431	0.9206	0.9132

Table 4. Analysis of variance (ANOVA) for CH_4 conversion.

Source	Sum of Squares	DF	Mean Square	F-value	p-value
Model	413.78	9	59.76	41.33	0.0051
A	552.98	1	552.98	222.20	0.0063
B	589.41	1	589.41	242.65	0.2557
C	556.78	1	556.78	118.38	0.0082
A^2	137.93	1	137.93	132.35	0.0004
B^2	187.38	1	187.38	125.84	0.0007
C^2	168.31	1	168.31	139.53	0.0001
AB	617.52	1	617.52	119.25	0.7326
AC	562.64	1	562.64	117.54	0.6791
BC	487.14	1	487.14	112.72	0.2604
Lack of Fit	158.98	3	52.99	73.84	0.0135

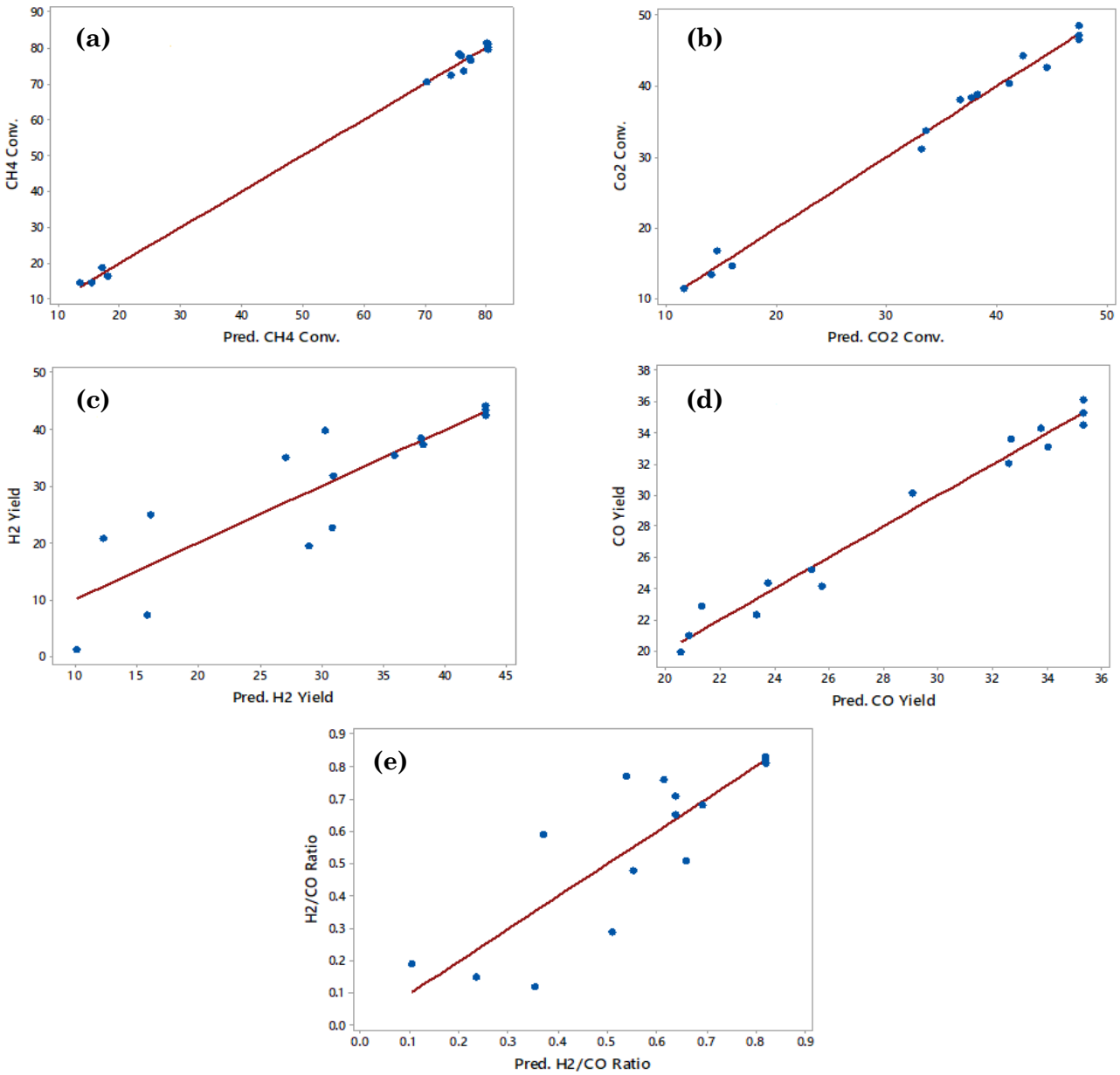

Figure 1. Actual and predicted values of (a) CH_4 conversion; (b) CO_2 conversion; (c) H_2 yield; (d) CO yield and (e) H_2/CO ratio.

Table 5. Analysis of variance (ANOVA) for CO_2 conversion.

Source	Sum of Squares	DF	Mean Square	F-value	p-value
Model	259.56	9	37.95	17.31	0.0039
A	131.59	1	131.59	263.20	0.0067
B	145.17	1	145.17	234.71	0.2438
C	133.49	1	133.49	128.51	0.0016
A^2	366.40	1	366.40	145.31	0.0032
B^2	334.77	1	334.77	116.67	0.0019
C^2	450.36	1	450.36	155.70	0.0001
AB	236.65	1	236.65	116.90	0.8765
AC	229.84	1	229.84	113.06	0.2053
BC	218.03	1	218.03	107.99	0.5656
Lack of Fit	38.40	3	12.79	32.59	0.0748

cients (A^2, B^2, and C^2) had significant impacts on the CO_2 and CH_4 conversions, H_2 and CO yields, and the syngas ratio of H_2 to CO (p less than 0.05), as shown in Tables 4 to 8. However, this implies that the interactive term coefficients (AB, AC, and BC) did not have a significant impact on the CO_2 and CH_4 conversions, H_2 and CO yields, and syngas ratio of H_2 to CO (p is more than 0.05) (Tables from 4 to 8). That means, the P and FR were remarkably affected by the linear terms of CO_2 and CH_4 conversions, and H_2/CO ratio, while R had the most

Table 6. Analysis of variance (ANOVA) for H_2 yield.

Source	Sum of Squares	DF	Mean Square	F-value	p-value
Model	416.04	9	57.34	28.48	0.0152
A	226.99	1	226.99	159.38	0.5661
B	222.28	1	222.28	123.20	0.3234
C	207.57	1	207.57	110.19	0.0002
A^2	470.22	1	470.22	125.34	0.0004
B^2	459.01	1	459.01	123.18	0.0002
C^2	384.34	1	384.34	120.71	0.0002
AB	223.77	1	223.77	116.67	0.8976
AC	237.01	1	237.01	112.77	0.6453
BC	211.93	1	211.93	120.10	0.4604
Lack of Fit	91.40	3	30.47	44.17	0.0223

Table 7. Analysis of variance (ANOVA) for CO yield.

Source	Sum of Squares	DF	Mean Square	F-value	p-value
Model	455.01	9	50.56	13.64	0.0054
A	120.07	1	120.07	169.02	0.8947
B	115.41	1	115.41	117.46	0.2815
C	101.10	1	101.10	127.28	0.0003
A^2	193.78	1	193.78	125.31	0.0005
B^2	127.10	1	127.10	117.32	0.0003
C^2	106.46	1	106.46	128.73	0.0001
AB	267.49	1	267.49	118.21	0.9865
AC	262.02	1	262.02	116.74	0.2574
BC	218.53	1	218.53	115.00	0.8797
Lack of Fit	17.15	3	5.72	8.30	0.1096

Table 8. Analysis of variance (ANOVA) for H_2/CO ratio.

Source	Sum of Squares	DF	Mean Square	F-value	p-value
Model	529.43	9	58.78	9.21	0.0124
A	146.21	1	146.21	265.33	0.5904
B	139.67	1	139.67	211.38	0.5635
C	130.03	1	130.03	240.48	0.0007
A^2	177.12	1	177.12	19.26	0.0074
B^2	198.78	1	198.78	12.16	0.0082
C^2	188.27	1	188.27	35.42	0.0002
AB	245.04	1	245.04	6.58	0.5098
AC	238.83	1	238.83	9.79	0.3753
BC	223.71	1	223.71	2.07	0.6321
Lack of Fit	32.03	3	11.75	15.75	0.1077

significant impact on H_2 and CO yields with a p-value is less than 0.05, as can be seen in Tables 4 to 8.

The quadratic terms of P, R, and FR were identified as significant parameters on the conversion of CO_2 and CH_4, yields of H_2 and CO, and the syngas ratio of H_2/CO (p-value less than 0.05) (Tables from 4 to 8). The interactive terms of P, R, and FR did not significantly influence the CO_2 and CH_4 conversions, H_2 and CO yields, and the syngas ratio of H_2 to CO with a p-value is less 0.05, as illustrated in Tables from 4 to 8. Therefore, all three factors (P, R, and FR) were found to have significant impacts on CO_2 and CH_4 conversions, H_2 and CO yields, and the syngas ratio of H_2 to CO (Tables 4 to 8)

However, for the conversions of CO_2 and CH_4 and syngas ratio of H_2/CO, the important factors were P and FR, followed by R, as shown in Tables 4 to 8. In contrast, for the yields of H_2 and CO, R had a greater effect than other factors, followed by P and FR (Tables 4 to 8). The synergistic effects of P-R, P-FR, and R-FR had a weak effect on the CO_2 and CH_4 conversions, H_2 and CO yields, and the syngas ratio of H_2 to CO because it had the lowest F-value (0.8765, 0.2053, and 0.5656 for CO_2 conversion; 0.7326, 0.6791, and 0.2604 for CH_4 conversion; 0.8976, 0.6453, and 0.4604 for H_2 yield; 0.9865, 0.2574, and 0.8797 for CO yield; and 0.5098, 0.3753, and 0.6321 for H_2 to CO syngas ratio, respectively), as shown in Tables 4 to 8.

The quadratic term coefficients of P, R, and FR on the CO_2 conversion, CH_4 conversion, H_2 yield, CO yield and H_2/CO ratio were more significant factors (0.0032, 0.0019, and 0.0001 conversion for CO_2; 0.0004, 0.0007, and 0.0001 conversion for CH_4; 0.0004, 0.0002, and 0.0001 yield for H_2; 0.0005, 0.0003, and 0.0001 yield for CO; and 0.0074, 0.0082, and 0.0001 for syngas ratio of H_2 to CO, respectively), as illustrated in Tables 2 to 8.

The 3-D response surfaces shown in Figures 2 to 6 (a, b, and c) are based on Equations (2 to 6) respectively, with one independent parameter kept at a fixed level which is (coded zero-levels), while the other 2 parameters were changed within the ranges of the experimental values. These figures show the effects of P and R, P and FR, and R and FR, respectively, on the conversions of CO_2 and CH_4, the yields of H_2 and CO, and the H_2/CO ratio.

The responses become better as the corresponding parameters increased until the maximum was reached. Afterwards, they continue to decrease even when both parameters still increasing, as presented in Figures from 2 to 6 (a, b, and c). For instance, Figures 2-6 (a and b) indicate that CO_2 and CH_4 conversions, H_2 and CO yields, and the ratio of H_2 to CO increase rapidly when P was extended from 8 to 10.5 W and then decreased a bit when P keep to increasing from 10.5 to 12 W. The reason for this behaviour might be the electron collisions for the molecules of CO_2 and CH_4 at 10.5 W till reaching the optimum value and then gradually declining with increasing P.

Previous studies [3,4,6–14] have shown that increasing input P leads to the development the electric field, the density of electrons, and the temperature of gas in the discharge zone [12]. When the residence time becomes shorter this will be translated to this situation CH_4

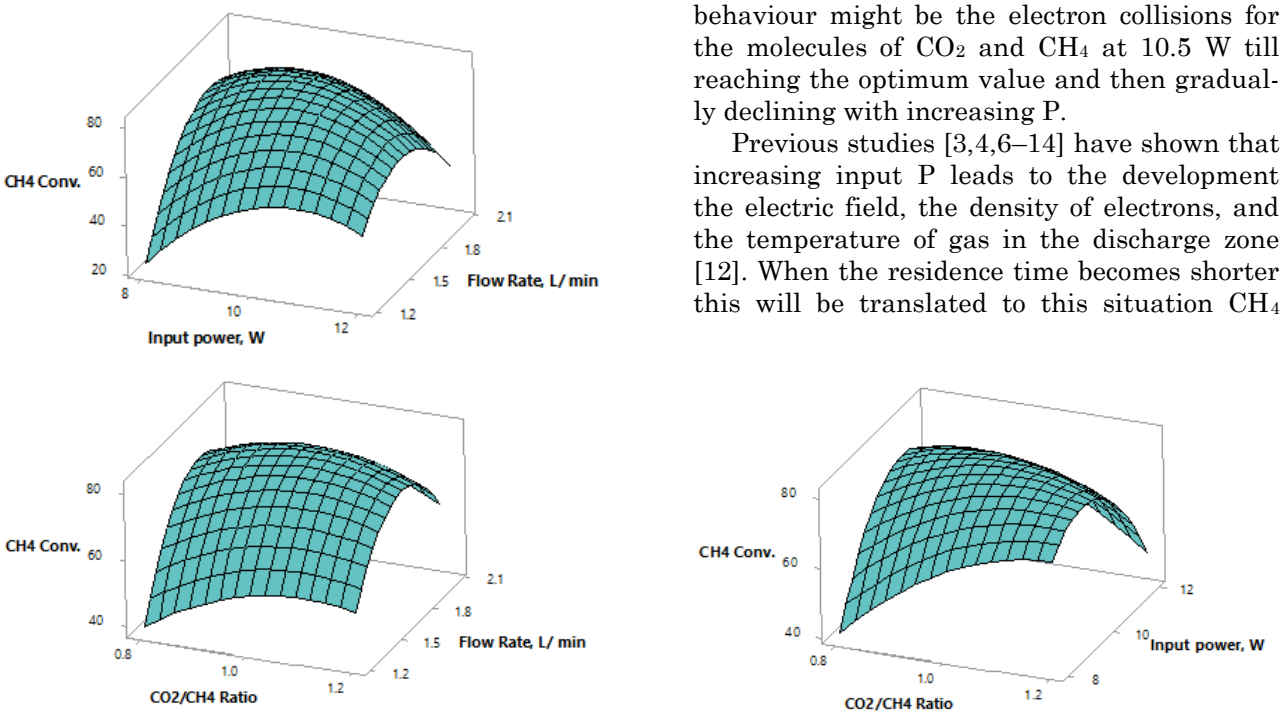

Figure 2. Effect of input power, CO_2/CH_4, and flow rate and their interaction on CH_4 conversion [(3D surface plots (a, b, and c)].

and CO_2 have shorter reaction times and fewer collisions with energetic species, such as electrons, OH, O, and O^-, leading to dissociation of CH_4 and CO_2 as represented by possible reactions listed in Equations (7) to (12) and Equations (13) to (18) for CH_4 and CO_2, respectively [15]. The initial reactions for CH_4 and CO_2 conversions are generally operated by electron-impact dissociation of CH_4 and CO_2, as shown in Equations (7) to (12). The CH_4 conversion to generate CH_3, CH_2, and CH as a reaction pathways exist (see Equations (7-11). These reactions are follow by radical recombination reactions to form higher hydrocarbons or electron-impact dissociation of radicals. When CH_4 and CO_2 are co-fed to a plasma reactor, they can promote the conversion of each other compared to CH_4 or CO_2 conversion pure [16]. The dissociation of CO_2 produced atomic oxygen species that can also break the C−H bond in CH_4 (see Equation 10), whereas the CH_4 dissociation produces hydrogen atoms that can help the CO_2 conversion (see Equation 13) [16].

After reaching the optimum value, the collision molecules of CO_2 and CH_4 decreased with increased P, as shown in Figures 2 to 6 (a and b). Therefore, the possibility of interaction molecules of CO_2 and CH_4 could be enhanced.

$$CH_4 + e \rightarrow CH_3 + H + e \quad (7)$$
$$CH_4 + e \rightarrow CH_2 + H_2 + e \quad (8)$$
$$CH_4 + e \rightarrow CH + H + H_2 + e \quad (9)$$
$$CH_4 + O \rightarrow CH_3 + OH \quad (10)$$
$$CH_4 + OH \rightarrow CH_3 + H_2O \quad (11)$$
$$CO_2 + e \rightarrow CO + O + e \quad (12)$$
$$CO_2 + H \rightarrow OH + CO \quad (13)$$

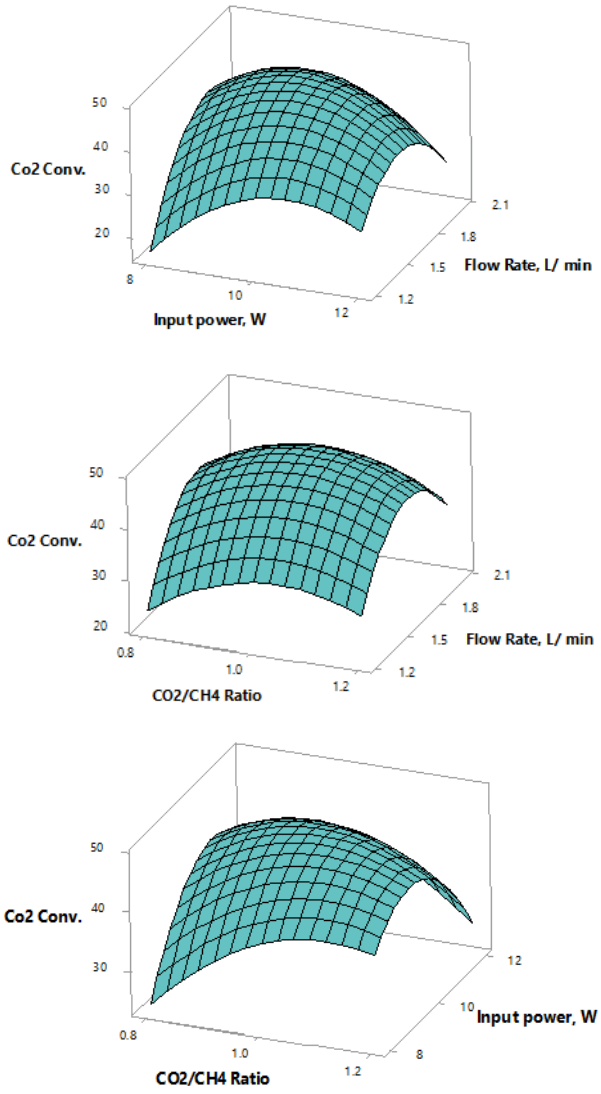

Figure 3. Effect of input power, CO_2/CH_4, and flow rate and their interaction on CO_2 conversion [(3D surface plots (a, b, and c)].

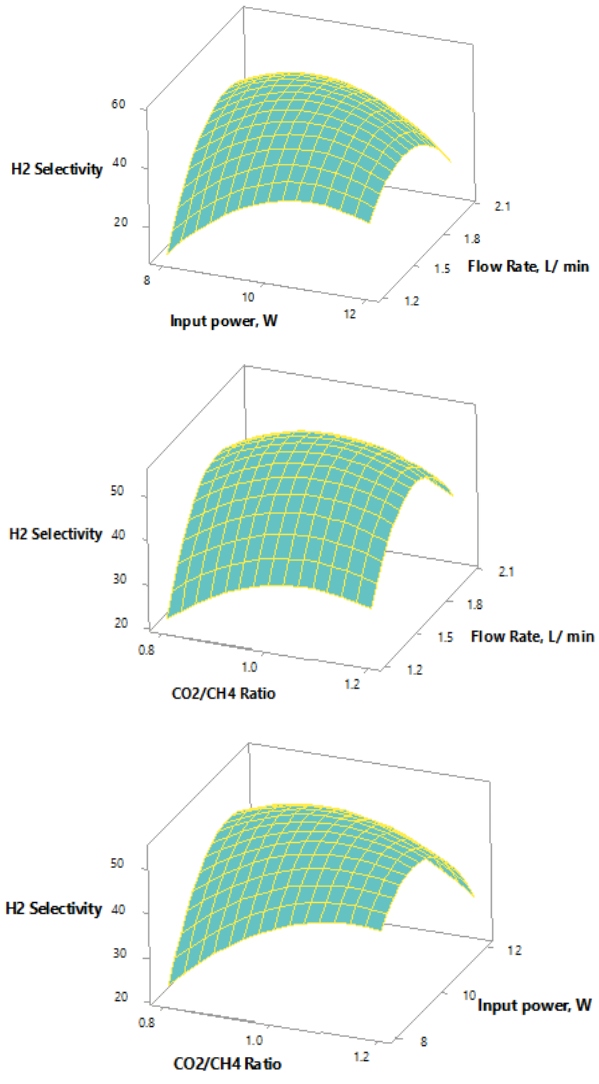

Figure 4. Effect of input power, CO_2/CH_4, and flow rate and their interaction on H_2 yield [(3D surface plots (a, b, and c)].

$CO_2 + e \rightarrow O + 2O + e$ (14)
$CO_2 + e \rightarrow CO + O^-$ (15)
$CO_2 + O \rightarrow CO + O_2$ (16)
$CO + O^- \rightarrow CO_2 + e$ (17)
$CO + O \rightarrow CO_2$ (18)

Similarly, the conversions of CO_2, CH_4, the yields of H_2, CO, and the ratio of H_2 to CO initially increased when R ranged from 0.8 to 1.03 and then decreased with increasing values of R from 1.03 to 1.2, as shown in Figures 2 to 6 (b and c). The reason for this behaviour could be that the number of collisions between the molecules of CO_2 and CH_4 increased until reaching the optimum value [16]. Afterwards, the collision interaction decreased with increased R, as shown in Figures 2 (b and c). Similar results have been reported by other researchers [10,17,19,20]. These transitions can be caused by increasing the initial concentration of CO_2, enhancing the collisions between the CO_2 and CH_4 molecules and the energetic electrons [13,21].

As depicted in Figures 2 to 6 (a and c), CO_2 and CH_4 conversions, H_2 and CO yields, and the syngas ratio of H_2 to CO increased with increasing FR from 1.2 to 1.58 L.min^{-1} and then declined with increased FR from 1.58 to 2 L.min^{-1}. The reason for this behaviour might be the residence time of the gas mixture molecules inside the discharge zone [19,22,24,26], which increased with escalated FR till reaching the highest value, and then started to decrease with increasing FR. This is consistent with previous studies [3,10,12,14,17,25,27,28].

Tables 4 to 8 respectively, indicate the F-values for the regression model for CO_2 conversion were 263.2076, 234.7125, and 128.5198; for CH_4 conversion were 222.2043, 242.6516, and 118.3809, for H_2 yield were 159.3832,

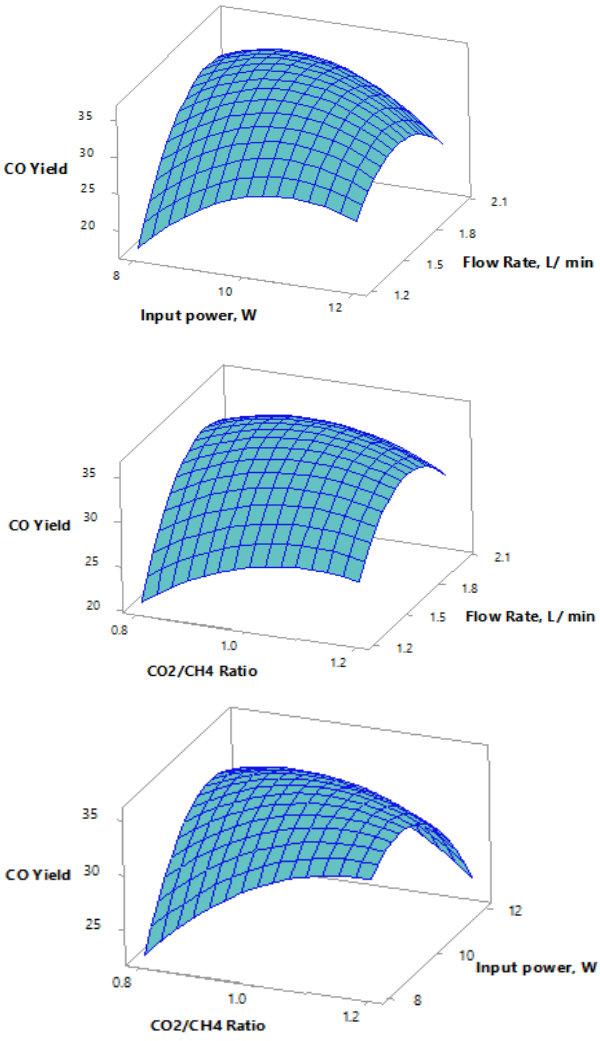

Figure 5. Effect of input power, CO_2/CH_4, and flow rate and their interaction on CO yield [(3D surface plots (a, b, and c)].

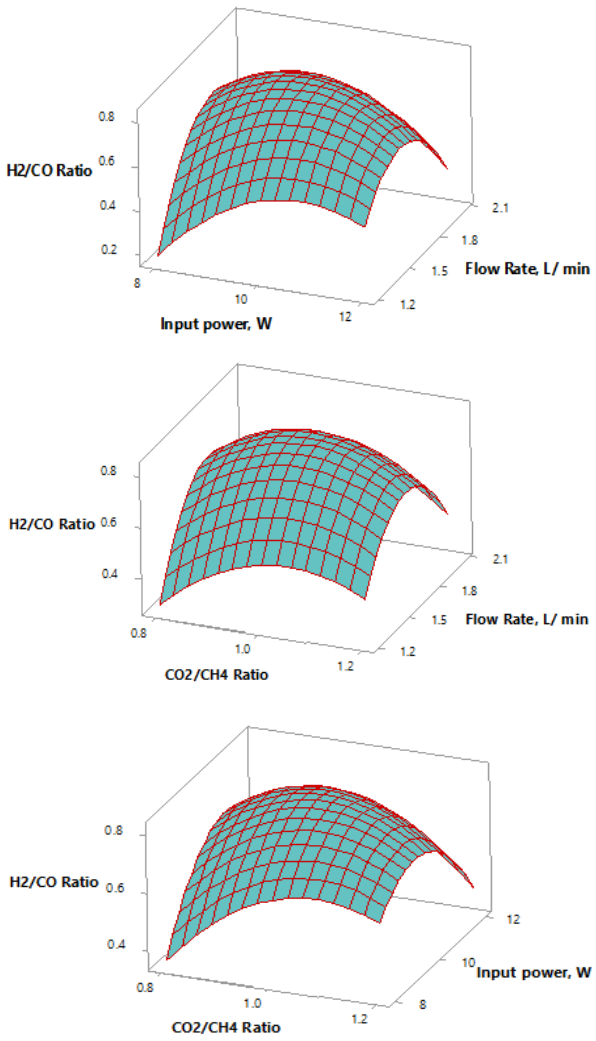

Figure 6. Effect of input power, CO_2/CH_4, and flow rate and their interaction on H_2/CO ratio [(3D surface plots (a, b, and c)].

123.2065, and 110.1989; for CO yield were 169.0267, 117.4609, and 127.2834; and for syngas ratio of H_2 to CO were 265.3321, 211.3876, and 140.0948, respectively.

The results of the F-value suggest that the model is statistically significant and represent the correlation between the input process factors and the plasma performance process. These results show that the regression model is adequate for the prediction and optimisation of the plasma H_2 and CO and yields.

3.3 Models Optimization and Validation

Lastly, the best operating values of the independent parameters for the production process of the synthesis gas were determined, and the fitting ability of predicting best responses values by models were calculated. The desirability function (DF) method was used to prove the optimal approaches to multiple responses. In addition, DF values are dimensionless, and the scale of desirability function ranges between (0 for unaccepted value of response and 1 for a desired value of response) [29]. The maximum desirable value of 0.97, and the optimal conditions of input P, R, and FR were 10.5 W, 1.03, and 1.58 L.min^{-1}, respectively, as shown in Figure 7. Under these conditions, the predicted responses of CO_2 and CH_4 conversions, H_2 and CO yield, and the syngas ratio of H_2 to CO were 48.56%, 86.67%, 45.87%, 39.43, and 0.88, respectively.

4. Conclusions

The present study was designed to determine the optimum conditions and investigate the synergistic effect of the P, R, and FR on the plasma stability and the synthesis gas production using a DBD plasma reactor system. The most obvious finding to emerge from this study is that the conversion of CO_2 and CH_4, the yield of the targeted products and the ratio of H_2 to CO were enhanced by synergistic effect of BBD. The results of this study indicate that using a DBD plasma reactor helps to reduce environmental problems and produce valuable compounds from CO_2 and CH_4. However, it would be interesting to assess the impact of integrating catalyst with DBD to enhance the conversions of CO_2 and CH_4 and the yield or selectivity of syngas.

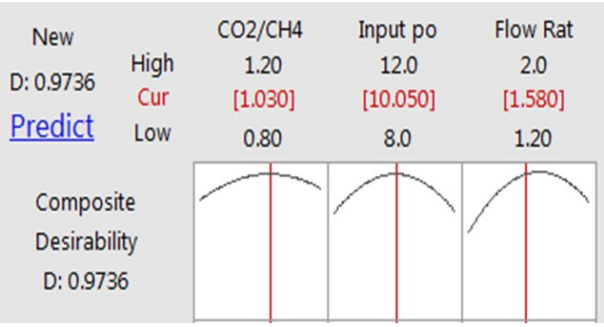

Figure 7. Desirability function applied for multiple responses.

Acknowledgment

The first author would like to thank the University of Technology, Baghdad, Iraq for their support in completing this research work.

CRediT Author Statement

Author Contributions: Nabil Alawi: Conceptualization, Methodology, Investigation, Resources, Data Curation, Writing. Hassan H. Al-Mohammedawi: Formal Analysis, Data Curation, Visualization, Software, Review and Editing. Firas Khaleel AL-Zuhairi, Hoang M. Nguyen, Jamal M. Ali: Review and Editing. All authors have read and agreed to the published version of the manuscript.

References

[1] Mei, D., Zhang, P., Duan, G., Liu, S., Zhou, Y., Fang, Z., Tu, X. (2022). CH_4 reforming with CO_2 using a nanosecond pulsed dielectric barrier discharge plasma. *Journal of CO2 Utilization*, 62, 102073. DOI: 10.1016/j.jcou.2022.102073.

[2] Alawi, N.M., Sunarso, J., Pham, G.H., Barifcani, A., Nguyen, M.H., Liu, S. (2020). Comparative study on the performance of microwave-assisted plasma DRM in nitrogen and argon atmospheres at a low microwave power. *Journal of Industrial and Engineering Chemistry*, 85, 118-129. DOI: 10.1016/j.jiec.2020.01.032.

[3] Aziznia, A., Bozorgzadeh, H.R., Seyed-Matin, N., Baghalha, M., Mohamadalizadeh, A. (2012). Comparison of dry reforming of methane in low temperature hybrid plasma-catalytic corona with thermal catalytic reactor over Ni/γ-Al_2O_3. *Journal of Natural Gas Chemistry*, 21(4), 466-475. DOI: 10.1016/S1003-9953(11)60392-7.

[4] Chun, S.M., Hong, Y.C., Choi, D.H. (2017). Reforming of methane to syngas in a microwave plasma torch at atmospheric pressure. *Journal of CO2 Utilization*, 19, 221-229. DOI: 10.1016/j.jcou.2017.03.016.

[5] Li, F., Ao, M., Pham, G.H., Jin, Y., Nguyen, M.H., Alawi, N.M., Liu, S. (2020). A novel UiO-66 encapsulated 12-silicotungstic acid catalyst for dimethyl ether synthesis from syngas. *Catalysis Today*, 355, 3-9. DOI: 10.1016/j.cattod.2019.07.057.

[6] Jiang, T., Li, Y., Liu, C.J., Xu, G.H., Eliasson, B., Xue, B. (2002). Plasma methane conversion using dielectric-barrier discharges with zeolite A. *Catalysis Today*, 72(3-4), 229-235. DOI: 10.1016/S0920-5861(01)00497-7.

[7] Moshrefi, M.M., Rashidi, F., Bozorgzadeh, H. R., Ehtemam Haghighi, M. (2013). Dry reforming of methane by DC spark discharge with a rotating electrode. *Plasma Chemistry and Plasma Processing*, 33, 453-466. DOI: 10.1007/s11090-013-9434-z.

[8] Ozkan, A., Dufour, T., Arnoult, G., De Keyzer, P., Bogaerts, A., Reniers, F. (2015). CO_2–CH_4 conversion and syngas formation at atmospheric pressure using a multi-electrode dielectric barrier discharge. *Journal of CO2 utilization*, 9, 74-81. DOI: 10.1016/j.jcou.2015.01.002.

[9] Qi, C., Wei, D., Xumei, T., Hui, Y., Xiaoyan, D., Yongxiang, Y. (2006). CO_2 reforming of CH_4 by atmospheric pressure abnormal glow plasma. *Plasma Science and Technology*, 8(2), 181. DOI: 10.1088/1009-0630/8/2/12.

[10] Shapoval, V., Marotta, E. (2015). Investigation on plasma-driven methane dry reforming in a self-triggered spark reactor. *Plasma Processes and Polymers*, 12(8), 808-816. DOI: 10.1002/ppap.201400177.

[11] Tu, X., Whitehead, J.C. (2012). Plasma-catalytic dry reforming of methane in an atmospheric dielectric barrier discharge: Understanding the synergistic effect at low temperature. *Applied Catalysis B: Environmental*, 125, 439-448. DOI: 10.1016/j.apcatb.2012.06.006.

[12] Tu, X., Whitehead, J.C. (2014). Plasma dry reforming of methane in an atmospheric pressure AC gliding arc discharge: Co-generation of syngas and carbon nanomaterials. *International journal of hydrogen energy*, 39(18), 9658-9669. DOI: 10.1016/j.ijhydene.2014.04.073.

[13] Wang, Q., Yan, B.H., Jin, Y., Cheng, Y. (2009). Investigation of dry reforming of methane in a dielectric barrier discharge reactor. *Plasma Chemistry and Plasma Processing*, 29, 217-228. DOI: 10.1007/s11090-009-9173-3.

[14] Zhang, A.J., Zhu, A.M., Guo, J., Xu, Y., Shi, C. (2010). Conversion of greenhouse gases into syngas via combined effects of discharge activation and catalysis. *Chemical Engineering Journal*, 156(3), 601-606. DOI: 10.1016/j.cej.2009.04.069.

[15] Chen, G., Silva, T., Georgieva, V., Godfroid, T., Britun, N., Snyders, R., Delplancke-Ogletree, M.P. (2015). Simultaneous dissociation of CO_2 and H_2O to syngas in a surface-wave microwave discharge. *International Journal of Hydrogen Energy*, 40(9), 3789-3796. DOI: 10.1016/j.ijhydene.2015.01.084.

[16] Zhou, L. M., Xue, B., Kogelschatz, U., Eliasson, B. (1998). Nonequilibrium plasma reforming of greenhouse gases to synthesis gas. *Energy & Fuels*, 12(6), 1191-1199. DOI: 10.1021/ef980044h.

[17] Zhang, S., Gao, Y., Sun, H., Fan, Z., Shao, T. (2022). Dry reforming of methane by microsecond pulsed dielectric barrier discharge plasma: Optimizing the reactor structures. *High Voltage*, 7(4), 718-729. DOI: 10.1049/hve2.12201.

[18] Zeng, Y., Zhu, X., Mei, D., Ashford, B., Tu, X. (2015). Plasma-catalytic dry reforming of methane over γ-Al_2O_3 supported metal catalysts. *Catalysis Today*, 256, 80-87. DOI: 10.1016/j.cattod.2015.02.007.

[19] Al-Mohammedawi, H.H., Znad, H., Eroglu, E. (2018). Synergistic effects and optimization of photo-fermentative hydrogen production of Rhodobacter sphaeroides DSM 158. *International Journal of Hydrogen Energy*, 43(33), 15823-15834. DOI: 10.1016/j.ijhydene.2018.06.140.

[20] Serrano-Lotina, A., Daza, L. (2014). Influence of the operating parameters over dry reforming of methane to syngas. *International Journal of Hydrogen Energy*, 39(8), 4089-4094. DOI: 10.1016/j.ijhydene.2013.05.135.

[21] Xu, Y., Tian, Z., Xu, Z., Lin, L. (2002). Reactions in a Mixture of CH_4 and CO_2 under the Action of Microwave Discharge at Atmospheric Pressure. *Journal of Natural Gas Chemistry*, 11(1/2), 28-32.

[22] Wu, A., Yan, J., Zhang, H., Zhang, M., Du, C., Li, X. (2014). Study of the dry methane reforming process using a rotating gliding arc reactor. *International journal of hydrogen energy*, 39(31), 17656-17670. DOI: 10.1016/j.ijhydene.2014.08.036.

[23] Pakhare, D., Spivey, J. (2014). A review of dry (CO_2) reforming of methane over noble metal catalysts. *Chemical Society Reviews*, 43(22), 7813-7837. DOI: 10.1039/C3CS60395D.

[24] Alawi, N.M., Nguyen, H.M. (2022). Discharge plasma reactor dry reforming of methane at high CO_2/CH_4 feed ratio. *AIP Conference Proceedings*, 2443(1), 030029. DOI: 10.1063/5.0092159.

[25] Timmermans, E.A.H., Jonkers, J.I.A.J., Thomas, I.A.J., Rodero, A., Quintero, M.C., Sola, A., Gamero, B., Van Der Mullen, J.A.M. (1998). The behavior of molecules in microwave-induced plasmas studied by optical emission spectroscopy. 1. Plasmas at atmospheric pressure. *Spectrochimica Acta Part B: Atomic Spectroscopy*, 53(11), 1553-1566. DOI: 10.1016/S0584-8547(98)00186-4.

[26] Long, H., Shang, S., Tao, X., Yin, Y., Dai, X. (2008). CO_2 reforming of CH_4 by combination of cold plasma jet and Ni/γ-Al_2O_3 catalyst. *International Journal of Hydrogen Energy*, 33(20), 5510-5515. DOI: 10.1016/j.ijhydene.2008.05.026.

[27] Li, L., Jiang, X., Wang, H., Wang, J., Song, Z., Zhao, X., Ma, C. (2017). Methane dry and mixed reforming on the mixture of bio-char and nickel-based catalyst with microwave assistance. *Journal of Analytical and Applied Pyrolysis*, 125, 318-327. DOI: 10.1016/j.jaap.2017.03.009.

[28] Pan, K.L., Chung, W.C., Chang, M.B. (2014). Dry reforming of CH_4 with CO_2 to generate syngas by combined plasma catalysis. *IEEE Transactions on Plasma Science*, 42(12), 3809-3818. DOI: 10.1109/TPS.2014.2360238.

[29] Chung, W.C., Chang, M.B. (2016). Dry reforming of methane by combined spark discharge with a ferroelectric. *Energy conversion and management*, 124, 305-314. DOI: 10.1016/j.enconman.2016.07.023.

[30] Ehrgott, M. (2005). *Multicriteria optimization* (Vol. 491). Springer Science & Business Media. DOI: 10.1007/978-3-662-22199-0.